

# Two qubit conditional quantum logic operation in a single self-assembled quantum dot

S. J. Boyle,<sup>1,\*</sup> A. J. Ramsay,<sup>1,†</sup> F. Bello,<sup>1</sup> H. Y. Liu,<sup>2</sup> M. Hopkinson,<sup>2</sup> A. M. Fox,<sup>1</sup> and M. S. Skolnick<sup>1</sup>

<sup>1</sup>*Department of Physics and Astronomy, University of Sheffield, Sheffield, S3 7RH, United Kingdom*

<sup>2</sup>*Department of Electronic and Electrical Engineering,  
University of Sheffield, Sheffield, S1 3JD, United Kingdom*

(Dated: February 29, 2008)

The four-level exciton/biexciton system of a single semiconductor quantum dot acts as a two qubit register. We experimentally demonstrate an exciton-biexciton Rabi rotation conditional on the initial exciton spin in a single InGaAs/GaAs dot. This forms the basis of an optically gated two-qubit controlled-rotation (CROT) quantum logic operation where an arbitrary exciton spin is selected as the target qubit using the polarization of the control laser.

PACS numbers: 78.67.Hc, 42.50.Hz, 03.67.Lx, 78.47.jp

Two qubit gates that operate on a ‘target’ qubit conditional on the state of the ‘control’ qubit, such as the controlled rotation (CROT) gate, provide the basic tool for entangling and disentangling qubits, and are therefore a critical component of any quantum processor [1]. One possible realization of a quantum processor is based on the use of semiconductor quantum dots, where the qubit is encoded in the presence or absence of an exciton, and manipulated using picosecond laser pulses. To date, considerable experimental progress has been made in the coherent optical control of a single exciton qubit [2, 3, 4, 5], and a two qubit gate has been reported for two excitonic qubits hosted in a single GaAs interface dot [6]. In the latter case, a CROT-gate is realized by driving a Rabi rotation on the exciton-biexciton transition, similar to proposals in ref. [7].

In this letter, we report on the conditional coherent optical control of two exciton qubits hosted in a single InGaAs/GaAs quantum dot. This is achieved by observing an exciton-biexciton Rabi rotation conditional on the initial state of the exciton spin, where the  $\pi$ -pulse acts as a controlled-rotation (CROT) gate. In contrast to ref. [6], we investigate the case of a CROT-gate where the polarization of the control laser is used to address both exciton-biexciton transitions simultaneously. In similar atomic systems arranged in a 3-level  $\Lambda$ -configuration, when two lasers are used to address each transition, arbitrary superpositions of the lower energy states can be coupled to the upper state [8]. In a quantum dot context, this provides a potential tool for selecting arbitrary exciton spin superpositions as the target and control qubits, providing a new degree of control over the two-qubit operation.

The experiments are performed on a single QD embedded in an n-i-Schottky diode structure, at a temperature of  $\sim 10$  K, full details of which can be found in ref. [9]. The dot is excited by up to two spectrally narrow laser pulses, with a Gaussian pulse shape and FWHM of 0.2 meV. A photocurrent detection method [3] is used, where under the action of an applied electric-field, the electron-hole pairs tunnel from the dot resulting

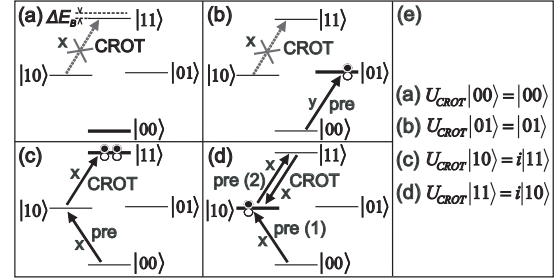


FIG. 1: Implementation of a CROT gate on two exciton-based qubits. The QD ground state  $|00\rangle$ , the two orthogonally polarized exciton ( $X^0$ ) states  $|01\rangle$ ,  $|10\rangle$ , the biexciton ( $2X^0$ ) state  $|11\rangle$ , and the biexciton binding energy  $\Delta E_B$  are indicated. The CROT operation is performed by an x-polarized  $\pi$ -pulse resonant with the  $X^0 - 2X^0$  transition. Cases (a)-(d) show the CROT operation on all four pure qubit states. (e) The CROT truth table.

in a change in the photocurrent.

The QD exciton-biexciton system may be considered as two excitonic-qubits labeled by their spin-states. There are 4 states: the ground state  $|00\rangle$ , two orthogonally polarized single exciton states  $|01\rangle$  and  $|10\rangle$ , and the biexciton state  $|11\rangle$ , as illustrated in fig. 1. The electron-hole exchange interaction causes the energy eigenstates of the exciton to be linearly polarized along the crystal lattice axes, designated the x and y axes. This results in strong selection rules for linear polarization and a fine structure splitting of  $10 - 100 \mu\text{eV}$ . Due to the Coulomb interaction, the ground state to exciton ( $0 - X^0$ ) and exciton to biexciton ( $X^0 - 2X^0$ ) transitions are separated by a biexciton binding energy  $\hbar\delta_B$ , of a few meV. The CROT operation flips the ‘target’ qubit if the ‘control’ qubit is in the  $|1\rangle$  state, according to the truth table shown in fig. 1(e). The gate can be realized by an x-polarized pulse with a pulse-area of  $\pi$ , resonant with the  $X^0 - 2X^0$  transition, labelled the CROT pulse. The effect of this pulse on all four pure qubit states is shown in fig. 1(a)-(d). (a) The dot is initially in the ground state  $|00\rangle$ . Hence the

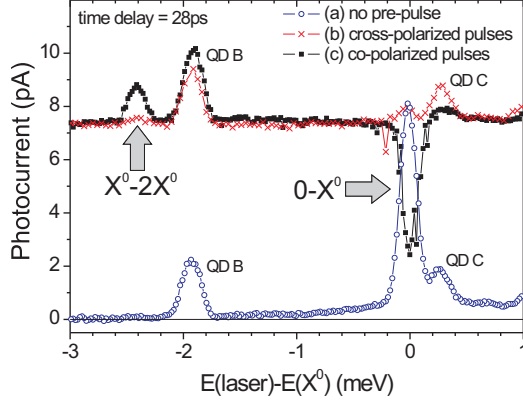


FIG. 2: Photocurrent spectra. (○) The single-pulse measurement shows the ground state to exciton transition ( $0 - X^0$ ) and two features from neighboring dots (QD B and QD C). For two-pulse measurements, a linearly polarized preparation pulse prepares the exciton state. (●) With co-polarized pulses, the exciton-biexciton transition ( $X^0 - 2X^0$ ) and quenching of the exciton are observed. (×) With cross-polarized pulses the ( $X^0 - 2X^0$ ) transition is suppressed by polarization selection rules.

CROT pulse is not resonant with any available transition and is not absorbed. (b) A y-polarized preparation pulse (pre-pulse) with a pulse area of  $\pi$ , resonant with the  $0 - X^0$  transition, precedes the CROT pulse, preparing the y-polarized exciton state  $|01\rangle$ . The CROT pulse is not absorbed due to polarization selection rules. (c) An x-polarized pre-pulse prepares the x-polarized exciton state  $|10\rangle$ , and the CROT pulse excites the  $|10\rangle \leftrightarrow |11\rangle$  transition. (d) Having prepared the  $|11\rangle$  state as in (c) using the first half of a  $2\pi$ -pulse, the second half of the pulse drives the system back to  $|10\rangle$ .

Single pulse and two-pulse measurements are made on a single QD with a  $0 - X^0$  transition energy of 1.302 eV, at a reverse bias of 0.6 V. In all measurements, ‘pre-pulse’ refers to a  $\pi$ -pulse resonant with the  $0 - X^0$  transition. The spectra in fig. 2 show photocurrent as a function of the detuning with respect to the  $0 - X^0$  transition of a  $\pi$ -pulse. (a) The single pulse measurement shows the  $0 - X^0$  transition. Two weak features, labelled B and C, are also observed due to the excitation of other nearby QDs. For two-color measurements, this pulse is preceded by the pre-pulse, which prepares an exciton state. Both pulses are linearly polarized along the crystal axes. (b) In the case of co-polarized pulses, an additional peak corresponding to the  $X^0 - 2X^0$  transition is observed at a detuning of  $\hbar\delta_B = -2.41$  meV [10]. At zero detuning a dip is observed, as the two pulses act as a  $2\pi$  Rabi rotation, first creating an exciton and then returning the dot to the ground state. (c) For cross-polarized pulses, polarization selection rules suppress the  $X^0 - 2X^0$  transition.

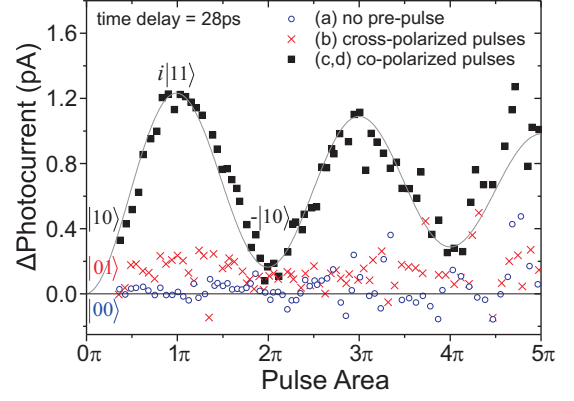


FIG. 3: Conditional exciton-biexciton ( $X^0 - 2X^0$ ) Rabi rotation (Change in photocurrent vs pulse area for a pulse resonant with the  $X^0 - 2X^0$  transition). (○) The single pulse measurement shows no oscillation, as the pulse is off-resonant, as in fig. 1(a). For two-pulse measurements, a linearly polarized preparation pulse prepares the  $X^0$  state. (●) With co-polarized pulses, a Rabi rotation between the  $X^0$  and  $2X^0$  states is observed, corresponding to fig. 1(c) and (d) for pulse areas of  $\pi$  and  $2\pi$  respectively. (×) Polarization selection rules suppress the Rabi rotation for cross-polarized pulses, as in fig. 1(b). The corresponding logic states are indicated.

To demonstrate the truth table of the CROT operation, we measure the  $X^0 - 2X^0$  Rabi rotation for all four pure qubit input states. Conditional Rabi rotation measurements are shown in fig. 3 as the change in photocurrent as a function of the pulse area of the CROT pulse, which is resonant with the  $X^0 - 2X^0$  transition and is polarized along one of the crystal axes. A background photocurrent, linear in power, is subtracted from all data. (a) The measurement without a pre-pulse shows a flat line, because the input state is the QD ground state  $|00\rangle$  and the CROT pulse is off-resonant, as in fig. 1(a). For two-color measurements, a pre-pulse, also polarized along one of the crystal axes, precedes the CROT pulse, preparing an exciton state. (b) In the measurement with cross-polarized pulses, an exciton is prepared polarized orthogonally to the control pulse, yielding an input state of  $|01\rangle$ . A flat response is measured, as polarization selection rules suppress the  $X^0 - 2X^0$  transition as in fig. 1(b). (c,d) With co-polarized pulses, an exciton is prepared with the same polarization as the control pulse. The input state is then  $|10\rangle$ , and more than two periods of a weakly damped Rabi rotation between the  $|10\rangle$  and  $|11\rangle$  states are observed. This corresponds to fig. 1(c) and 1(d) for pulse areas of  $\pi$  and  $2\pi$  respectively. These experiments demonstrate the truth table of the CROT gate for pure qubit input states.

In the long term, high-fidelity gates will be needed to realize fault-tolerant quantum information processing. It is therefore useful to evaluate the performance of this CROT gate in an InAs dot, and compare it to that with

a GaAs dot [6]. Since the potential coherence times of InAs dots are far superior to GaAs dots (600 ps [11] versus 50 ps [6]), much higher gate fidelities are expected. One feasible comparison is to calculate the fidelity using experimentally determined parameters in a 4-level atom model as described in the supplementary information of ref. [6]. For the data presented in fig. 3, the exciton coherence time is limited by electron tunnelling to  $T_2 = 130 \pm 20$  ps, giving a fidelity of  $0.87 \pm 0.04$ , compared to 0.7 for GaAs interface dots where  $T_2$  is limited by the radiative lifetime to 46 ps [6]. If a similar calculation is made using state-of-the-art values for photocurrent detection with InAs dots (laser bandwidth 0.4 meV,  $T_2 = 320$  ps) [5] a fidelity of 0.97 is in prospect. We note that in the region of interest (pulse-area  $\Theta < 2\pi$ ) the model is in good agreement with the Rabi rotation data, where the signal at  $2\pi$  returns to its value at  $0\pi$  to within 15%. However, the model does not account for intensity damping effects [12], and should therefore be treated cautiously. Overall, the comparison supports the expectation that much higher fidelity quantum gates are possible with InAs dots compared with GaAs dots.

The polarization of the control laser may be used to drive both exciton-biexciton transitions simultaneously, and by analogy with similar atomic  $\Lambda$ -transitions [8], should provide an additional degree of control over the two-qubit operation. We thus present a study of the polarization properties of the exciton-biexciton Rabi rotation. We consider the case of two laser pulses, designated (1) and (2), with carrier frequencies on-resonance with the  $(0 - X^0)$  and  $(X^0 - 2X^0)$  transitions respectively. Both pulses are spectrally narrow so that they excite only one set of transitions. The control Hamiltonian in the rotating frame of the states  $|00\rangle, |\uparrow\rangle, |\downarrow\rangle, |11\rangle$ , where the spin up/down exciton states  $\uparrow/\downarrow$  are used for ease of presentation, is given by:

$$\hat{H} = \frac{1}{2} \begin{pmatrix} 0 & \Omega_+^{(1)} & \Omega_-^{(1)} & 0 \\ \Omega_+^{(1)*} & 0 & \delta_{fs} & \Omega_-^{(2)} \\ \Omega_-^{(1)*} & \delta_{fs} & 0 & \Omega_+^{(2)} \\ 0 & \Omega_-^{(2)*} & \Omega_+^{(2)*} & 0 \end{pmatrix}$$

where  $\hbar = 1$ , and  $\delta_{fs}$  is the fine-structure splitting, and  $\Omega_{\pm}^{(\alpha)}$  are the  $\sigma_{\pm}$  circularly polarized components of the complex Rabi frequency of each laser. For the sake of clarity, we neglect coherence loss. If the pulses have no spectral or temporal overlap, and are much shorter than the fine-structure period, the control Hamiltonian may be interpreted as a time-sequence of rotations  $\hat{U}_{\gamma}$ .

For the pre-pulse the control Hamiltonian reduces to:

$$\hat{H}_1 = \frac{1}{2} |00\rangle [\Omega_+^{(1)} |\uparrow\rangle + \Omega_-^{(1)} |\downarrow\rangle] + h.c. \equiv \frac{\Omega_1}{2} |00\rangle \langle A_1| + h.c.$$

where  $\Omega_{\alpha} = \sqrt{|\Omega_+^{(\alpha)}|^2 + |\Omega_-^{(\alpha)}|^2}$  is the effective Rabi frequency of pulse  $(\alpha)$ . Here the vacuum-exciton transitions

form a 3-level V-configuration [13]. The pre-pulse drives a Rabi rotation between the vacuum state  $|00\rangle$  and the exciton-spin superposition state  $|A_1\rangle$  labelled the “active” state, leaving the orthogonal “inactive” state  $|\bar{A}_1\rangle$  untouched. Hence the full polarization of a pre-pulse with pulse-area of  $\pi$  is imprinted on the exciton spin.

During the inter-pulse time interval the fine-structure drives a rotation  $\hat{U}_{fs}$  between exciton spin up and down states [14]. For the CROT pulse the control Hamiltonian reduces to:

$$\hat{H}_2 = \frac{1}{2} [\Omega_-^{(2)} |\uparrow\rangle + \Omega_+^{(2)} |\downarrow\rangle] \langle 11| + h.c. \equiv \frac{\Omega_2}{2} |A_2\rangle \langle 11| + h.c.$$

Here the exciton-biexciton transitions form a 3-level  $\Lambda$ -configuration, where the CROT pulse drives a Rabi rotation between the “active” exciton spin superposition state  $|A_2\rangle$ , and the biexciton state  $|11\rangle$ , leaving the “inactive”  $|\bar{A}_2\rangle$  state untouched. In essence the polarization can select any arbitrary exciton spin as the ‘target’  $|\bar{A}_2\rangle$  and ‘control’  $|A_2\rangle$  qubits, and this can be used as a control tool. For example, the polarization of a CROT pulse with a pulse-area of  $\pi$  can select an exciton spin superposition to project into the biexciton state, providing a means of detecting the exciton spin. Alternatively, full optical control of the exciton spin can be achieved as follows. A CROT-pulse with a pulse-area of  $2\pi$  imparts a detuning-dependent phase-shift of up to  $\pi$  [15, 16] on  $|A_2\rangle$  with respect to  $|\bar{A}_2\rangle$ , and since any exciton spin superposition may be selected as  $|A_2\rangle$ , full optical control of the exciton spin can be achieved using the polarization of the pulse [13]. This results in a gate time limited by the duration of the control pulse, far faster than two-pulse techniques where the exciton spin is controlled using the fine-structure beat [2, 5].

To test this model, we study the dependence of the  $0 - X^0$ , and  $X^0 - 2X^0$  Rabi rotations on the polarizations of the pre and CROT pulses. Figure 4(d) shows a Poincaré sphere representation of the polarization where  $(\Omega_+, \Omega_-) = \Omega(e^{i\alpha} \cos \beta, e^{-i\alpha} \sin \beta)$ . The period of the  $0 - X^0$  and  $X^0 - 2X^0$  Rabi rotations are independent of polarization. For time-resolved measurements (not shown), where both the pre and CROT pulses are  $\pi$ -pulses, fine-structure beats with a period of 320 ps are observed.

To test that the CROT-pulse drives a Rabi rotation between the “active” exciton spin superposition  $|A_2\rangle$  and the biexciton  $|11\rangle$  states, we measure the amplitude of the Rabi rotation as a function of the polarization of the CROT pulse, in both the linear and elliptical planes of the Poincaré sphere (fig. 4d), and compare with the model:  $\Delta PC \propto |\langle A_2 | \hat{U}_{fs} | A_1 \rangle|^2$ .

(*Linear plane*) The pre-pulse is linearly polarized along the x-axis, to excite an energy eigen-state, and the Rabi rotations are measured as a function of linear polarization  $\alpha_{crot}$  with  $(\alpha_{pre} = 0, \beta_{pre} = \beta_{crot} = +45^\circ)$ . Figure 4(a)

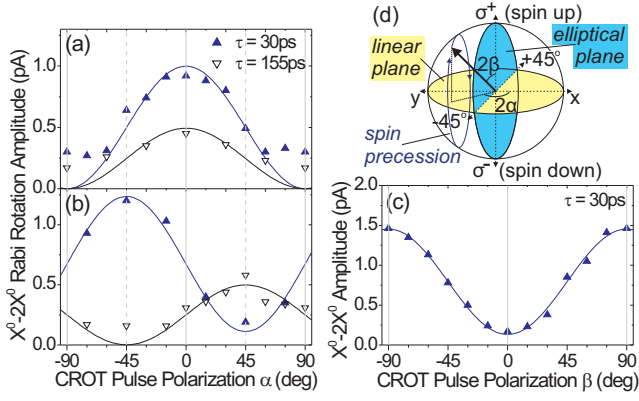


FIG. 4: Amplitude of the  $X^0 - 2X^0$  Rabi rotation measured as a function of the polarization of the CROT pulse. (a,b) Linearly polarized CROT-pulse probes exciton created with (a)  $x$ , (b)  $-45^\circ$  linearly polarized pre-pulse. (c) An elliptically polarized CROT-pulse probes exciton created by  $\sigma_+$  polarized pre-pulse. Full lines (a)-(c), are fits to data using:  $\Delta PC \propto |\langle A_2 | \hat{U}_{fs} | A_1 \rangle|^2$ . (d) Poincaré sphere representation of exciton spin, with spin precession due to fine structure.

presents the results. A cosine dependence is observed where maximum signal occurs when the pulses are co-linearly polarized. This is true for all time-delays since there is no precession of the exciton spin. Next, for the results presented in fig. 4(b), a  $-45^\circ$  linearly polarized pre-pulse is used, and the amplitude recorded as a function of the CROT linear polarization ( $\alpha_{pre} = -45^\circ, \beta_{pre} = \beta_{crot} = +45^\circ$ ). At short time-delay ( $\delta_{fs}\tau < \pi/2$ ) maximum signal again occurs for co-linearly polarized excitation. However, at  $\tau = 155$  ps the maximum now occurs for cross-linear polarization due to the fine-structure rotation. In fig. 4(a-c) the solid-lines show the good fits to data using  $\Delta PC \propto |\langle A_2 | \hat{U}_{fs} | A_1 \rangle|^2$ , where the amplitudes of the oscillations are the only fitting parameters.

(*Elliptical plane*) To probe the elliptically polarized plane, a circularly polarized pre-pulse is used ( $\alpha_{pre} = \alpha_{crot} = 45^\circ, \beta_{pre} = 0$ ), and the amplitude of the Rabi rotation measured as a function of the ellipticity angle of the CROT-pulse  $\beta_{crot}$ . At short time-delay, the maximum is observed for cross-circular excitation, see fig.4(c). The measurements show close agreement with the model for both planes of the Poincaré sphere, implying that the full polarization of the pre-pulse is stored in the exciton spin, and then a selected component is projected into the biexciton state by the CROT-pulse. This further implies that the polarization of the CROT pulse selects an exciton spin superposition to couple optically to the biexciton state.

In conclusion, we have demonstrated a CROT quantum logic gate for two excitonic qubits in a single In-GaAs/GaAs dot, with a high fidelity of  $0.87 \pm 0.04$ . Furthermore, we find that the polarization of the control

pulse may be used to select arbitrary exciton spin superpositions as the target and control qubits. This property may be used to construct an operator which combines elements of the CROT and bit-swap operations into a single control pulse, offering a more efficient control sequence than a series of CROT and single qubit operations.

This work was funded by EPSRC UK GR/S76076 and the QIPIRC UK.

\* Electronic address: s.boyle@shef.ac.uk

† Electronic address: a.j.ramsay@shef.ac.uk

- [1] A. Barenco, D. Deutsch, A. Ekert, and R. Jozsa, Phys. Rev. Lett. , **74** 4083 (1995).
- [2] N. H. Bonadeo, J. Erland, D. Gammon, D. Park, D. S. Katzer, and D. G. Steel, Science **282** 1470 (1998).
- [3] A. Zrenner, E. Beham, S. Stuffer, F. Findeis, M. Bichler, and G. Abstreiter, Nature **418**, 612 (2002).
- [4] T. H. Stievater, Xiaoquin Li, D. G. Steel, D. Gammon, D. S. Katzer, D. Park, C. Piermarocchi, and L. J. Sham Phys. Rev. Lett. **87**, 133603 (2001).
- [5] S. Stuffer, P. Ester, A. Zrenner, and M. Bichler, Phys. Rev. B **72** 121301(R) (2005).
- [6] X. Li, Y. Wu, D. G. Steel, D. Gammon, T. H. Stievater, D. S. Katzer, D. Park, C. Piermarocchi, and L. J. Sham Science **301**, 809 (2003).
- [7] E. Biolatti, R. C. Iotti, P. Zanardi, and F. Rossi, Phys. Rev. Lett. , **85** 5647 (2000).
- [8] P. Král, I. Thanopoulos, and M. Shapiro, Rev. Mod. Phys. **79** 53 (2007).
- [9] R. S. Kolodka, A. J. Ramsay, J. Skiba-Szymanska, P. W. Fry, H. Y. Liu, A. M. Fox, and M. S. Skolnick, Phys. Rev. B **75** 193306 (2007).
- [10] The photocurrent detection efficiency is limited by the hole tunneling rate [9]. Hence the  $X^0 - 2X^0$  signal, which involves tunnelling of two holes, is weaker than  $0 - X^0$  at this bias.
- [11] P. Borri, W. Langbein, S. Schneider, U. Woggon, R. L. Sellin, D. Ouyang, and D. Bimberg, Phys. Rev. Lett. **87**, 157401 (2001).
- [12] Q. Q. Wang, A. Muller, P. Bianucci, E. Rossi, Q. K. Que, T. Takagahra, C. Piermarocchi, A. H. MacDonald, and C. K. Shih, Phys. Rev. B , **72** 035306 (2005).
- [13] Q. Q. Wang, A. Muller, M. T. Cheng, H. J. Zhou, P. Bianucci, and C. K. Shih, Phys. Rev. Lett. **95** 187404 (2005). In this work, an exciton spin-flip was demonstrated using a  $2\pi$ -pulse to drive both vacuum-exciton transitions.
- [14] A. I. Tartakovskii, J. Cahill, M. N. Makhonin, D. M. Whittaker, J-P. R. Wells, A. M. Fox, D. J. Mowbray, M. S. Skolnick, K. M. Groom, M. J. Steer and M. Hopkinson, Phys. Rev. Lett. **93** 057401 (2004).
- [15] A. J. Ramsay, S. J. Boyle, R. S. Kolodka, J. B. B. Oliveira, J. Skiba-Szymanska, H. Y. Liu, M. Hopkinson, A. M. Fox, and M. S. Skolnick, cond.mat: 0710.3738 (2007).
- [16] S. E. Economou, and T. L. Reinecke, Phys. Rev. Lett. , **99** 217401 (2007).